Numerical study on kerosene spray in supersonic flow

L.J. Yue and G. Yu

LHD, Institute of Mechanics, Chinese Academy of Sciences, Beijing 100080, China

Abstract. Numerical simulation was conducted to study the kerosene spray characteristics injecting into supersonic cross flow. The verification of the simulation was carried out by experimental Schlieren image. Furthermore, the aerodynamic secondary breakup effect of the supersonic cross flow on the initial droplets was investigated. It was revealed that the initial parent drops were broken up into small drops whose diameter is about O(10) micrometers soon after they entered into the supersonic cross flow. During the appropriate range of initial drop size, the parent droplets would be broken up into small drops with the same magnitude diameter no matter how large the initial drops size was.

1 Nomenclature

c_d	Liquid specific heat	$\vec{u}$	Fluid velocity
C_D	Aerodynamic drag coefficient of liquid drop	$\vec{u}'$	Gas turbulence velocity
		$\vec{v}_p$	Droplet velocity
C_{DS}	Drag coefficient of rigid sphere	V_r	Initial relative velocity
D	Diffusion coefficient	Y_1^*	Kerosene vapor mass fraction at droplet's surface
$\vec{g}$	Gravitational acceleration		
$L(T_d)$	Latent heat of vaporization	ν	Distortion parameter of drop surface oscillation
Q_d	Rate of the heat conduction to the drop surface per unit area	ρ	Gas density
		ρ_d	Liquid density
r	Droplet radius	k	Turbulence kinetic energy
We	Weber number	ε	Turbulence kinetic energy dissipation
s_{ij}	Mean stress rate tensor	μ	Gas viscosity
Sh_d	Sherwood number for mass transfer	μ_l	Viscosity of the liquid fuel
t_{bu}	Drop breakup time	σ	Surface tension
T_d	Droplet temperature		

2 Introduction

As compared to hydrogen, liquid hydrocarbons, such as kerosene, are attractive candidates for fueling the scramjet in the lower hypersonic flight regime of $M < 8$ [1]. However, up to now, the complex spray phenomena can't be understood well due to the limit of experimental measurement technique. Additionally, numerical simulations were seldom found in the literatures.

A modified code was developed by the author based on KIVA-3 to simulate liquid spray in supersonic flow[2]. KIVA is a code written for internal combustion engine, which can analyze transient, three-dimensional, multiphase, and multi-component flow including chemically reaction with spray[3]. Although spray models, the boundary conditions, special specifications and mesh generation are designed for IC engine, its equations and solution procedure possess generality, and the range of validity of the code can extends from low speeds to supersonic flows with laminar and turbulent regimes. So some necessary modifications can be made to simulate the spray in supersonic flow.

The objective of present research is to study spray characteristics and the secondary breakup effect of the supersonic cross flow on the initial droplets based on the modified code.

3 Numerical models and methods

A stochastic particle method is used to calculate the liquid sprays, in which transport of the dispersed phase is calculated by tracking the trajectories of a certain number of representative parcels. Various sub-models account for the effects of turbulent dispersion, droplet collisions, evaporation and aerodynamic breakup. The mass, momentum, and energy exchange between the spray and the gas is also taken into account by adding source terms into the gas equations.

3.1 Turbulence model

In order to account for the effects of compressibility, RNG $k-\varepsilon$ model was used, and a new term S_R was introduced in the ε equation.

$$S_R = -\frac{c_\mu \eta^3 (1-\eta/\eta_0)}{1+\beta\eta^3}\rho\frac{\varepsilon^2}{k} \tag{1}$$

$$\eta = S\frac{k}{\varepsilon}, \qquad S = 2(s_{ij}s_{ij})^2$$

Where, $\eta_0 = 4.38$, $\beta = 0.012$ [4].

3.2 Motion of droplets

The effect of aerodynamic drag and gravitational force on droplet acceleration was considered, as shown in Eq.(2).

$$\frac{d\vec{v}}{dt} = \frac{3}{8}\frac{\rho}{\rho_d}\frac{|\vec{u}+\vec{u}'-\vec{v}_p|}{r}(\vec{u}+\vec{u}'-\vec{v}_p)C_D + \vec{g} \tag{2}$$

3.3 TAB breakup model

The TAB breakup model considers a liquid drop to be analogous to a spring-mass system (Taylor's analogy)[5]. The oscillation of the drop surface is described by a second order ordinary differential equation:

$$\ddot{y} = \frac{2}{3}\frac{\rho}{\rho_d}\frac{(\vec{u}+\vec{u}'-\vec{v}_p)^2}{r^2} - \frac{8\sigma}{\rho_d r^3}y - \frac{5\mu_l}{\rho_d r^2}\dot{y} \tag{3}$$

In which, y is proportional to the displacement of the equator of the droplet from its equilibrium position, divided by half droplet radius. The drop breakup is due to an increase in the amplitude of the drop oscillation. Breakup occur if and only if $y \geq 1$.

3.4 Turbulent dispersion of droplets

The dispersion of droplets due to gas phase turbulence is modeled by adding to the gas velocity a fluctuating velocity $\vec{u}'$, each component $\vec{u}'$ follows a Gaussian distribution with mean square deviation $2/3\,k$,

$$G(\vec{u}') = (4/3\pi k)^{-1/2}\exp\{-3|\vec{u}'|^2/4k\} \tag{4}$$

The sampled fluctuating velocity is applied over the turbulence correlation time, which is the minimum of the eddy breakup time and a time for the droplet to traverse the eddy.

3.5 Droplet evaporation

The rate of droplet radius change is given by the Frossling correction

$$\frac{dr}{dt} = -\frac{(\rho D)_{air}(\hat{T})}{2\rho_d r}\frac{Y_1^* - Y_1}{1 - Y_1^*}Sh_d \tag{5}$$

The temperature of the droplet can be determined by the energy balance equation

$$\rho_d \frac{4}{3}\pi r^3 C_d \frac{dT_d}{dt} - \rho_d 4\pi r^2 \frac{dr}{dt}L(T_d) = 4\pi r^2 Q_d \tag{6}$$

3.6 Droplet drag coefficient

In compressible flows, the drag coefficient of the rigid sphere CDS was calculated based on the local relative Mach number[6].

However, the drops undergo significant flattening and no longer spherical as soon as they enter the air flow. Therefore, the drag coefficient of a distorting drop should be a function of distortion parameter and lie between that of a rigid sphere and that of a disk. It was found that the drag coefficient of sphere in a compressible flow is about 1 and is approximate 1.5 for rigid disk[7]. By using the distortion parameter y in the TAB model, a simple expression was proposed.

$$C_D = C_{DS}(1 + 0.5y) \tag{7}$$

Furthermore, the frontal area of the drop exposed to the flow is also changed due to its distortion, which is expressed below.

$$A_f = \pi r^2 * (1 + y/2)^2 \tag{8}$$

3.7 Droplet collision and coalescence

The basic assumptions are that the number of droplets associated with each drop particle is distributed in the computational cell, and the collision calculation is performed for the pair of particles only if they are in the same computational cell. The collision frequency can be calculated, and then be used to solve the probability that a droplet will undergo a collision with a drop in the other particles.

3.8 Numerical technique

The solution procedure was based on ALE method. In the Lagrangian phase, the mesh vertices move with the gas velocity, and there is no convection across cell boundaries. Spray droplet collision, evaporation and breakup terms are calculated. Meanwhile, mass and energy source terms due to spray are treated by explicit scheme. Implicit differencing is then used for all the diffusion terms and the terms associated with pressure wave propagation of the gas equations as well as the spray momentum source term. The coupled implicit equations are solved by a method similar to the SIMPLE algorithm, with individual equation being solved by the conjugate residual method. In the rezone phase, the flow field is frozen and remapped onto new computational mesh. Explicit methods are used to calculate convection, which is subcycled several times due to the restriction of Courant stability condition.

3.9 Boundary conditions

All the parameters at the entrance of computational domain were given. The combustor wall was considered to be adiabatic and a wall function was employed. The flow variables at outflow boundaries were determined by 1st-order extrapolation from the computational domain.

The dispersed phase may be introduced anywhere within the flow domain, at which droplet mass flow rate and distribution of droplet sizes, velocity, temperature, cone angle and oscillation parameters were specified.

4 Results and discussions

Simulation was conducted to study the kerosene spray injecting through the 0.8mm wall orifice into the Mach 2.5 cross flow with the static temperature of 430K and static pressure of 0.043MPa. Fuel was injected at 2.2MPa, 300K. In present work, the surrogate fuel model $C_{12}H_{24}$ was proposed as a generic representation for kerosene[8].

4.1 Analysis and comparison with Schlieren image

In the calculation, the initial Sauter Mean Radius (SMR) of the drops was given 35mm based on the measurement at the 70mm downstream of the injecting orifice by PDA in case of kerosene injecting into quiescent atmosphere.

Fig.1(a) and (b) demonstrate the numerical spray structure and pressure contour. In Fig.1(a), the color denotes the droplet size. It is found that a bow shock wave appears upstream of the injector due to the obstruction of the liquid jet. Meanwhile, Spray is severely bent by the gas flow. Smaller droplets have lower inertia and more quickly follow with the gas flow, thus larger droplets are at the periphery of spray. Furthermore, the crimped spray plume reveals the influence of the turbulent diffusion.

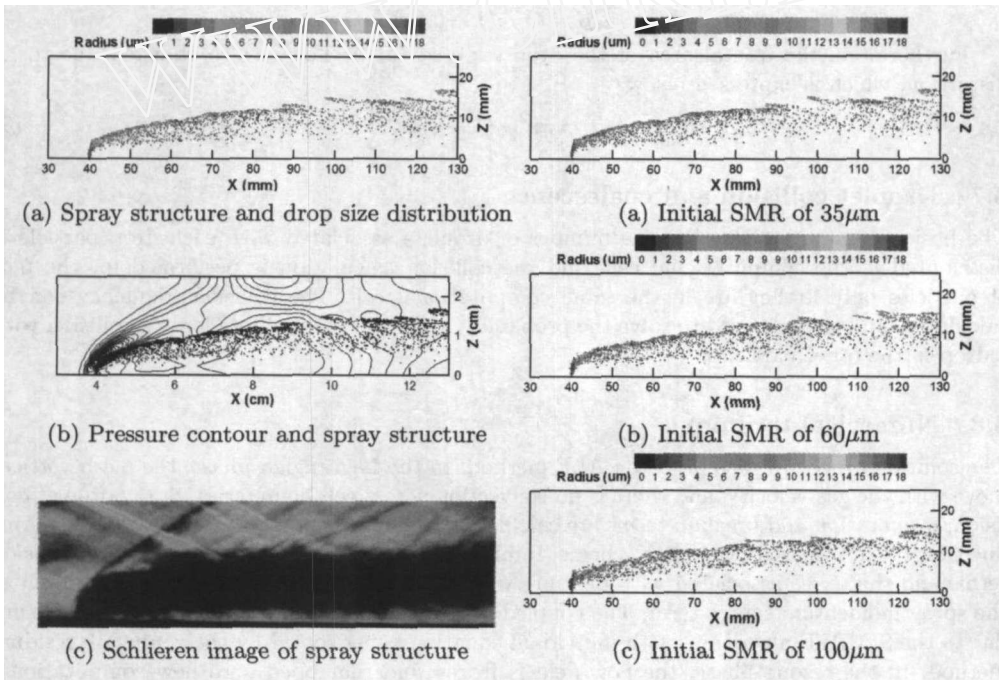

Fig. 1. Numerical and experimental kerosene spray, P_f = 2.2MPa d_0 = 0.8mm

Fig. 2. Spray structure and drop size distribution with different initial drop SMR, (P_f = 2.2MPa d_0 = 0.8mm)

In order to verify the numerical simulation, the corresponding visualization images of the kerosene spray was taken by schlieren, as shown in Fig.1(c). Through the comparison, the numerical and experimental kerosene spray plumes showed good agreement.

Fig.3 further quantitatively shows the variation of the average SMR of droplets at the cross section with axial location. It is clear that initial parent drops are broken up into small drops

whose diameter is about O(10) micrometers soon after they enter into the supersonic cross flow. It may be attributed to the effect of secondary breakup. Because the Weber number of the droplet issued from the injector into the supersonic cross flow is over 1000, then the so-call 'catastrophic' breakup phenomenon will occur[9].

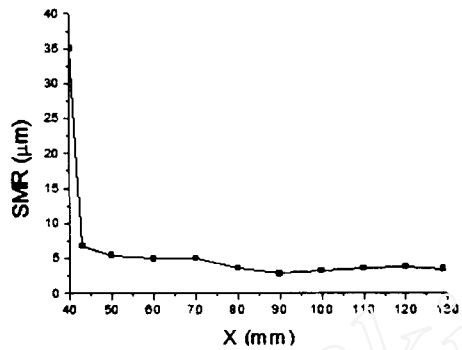

Fig. 3. Variation of average SMR of droplets at the cross section with axial location

Pilch had deeply investigated the breakup of a liquid drop in the gas flow[10]. Total breakup time for low-viscosity drops are given by:

$$t_{bu} = T\sqrt{\rho_d/\rho}2r/V_r \tag{9}$$

Here, T is a dimensionless time characteristic of drop breakup by Rayleigh-Taylor or Kelvin-Helmholtz instability.

$$\begin{aligned} T &= 0.766(We-12)^{0.25},\ 351 \le We \le 2670 \\ T &= 5.5, \qquad\qquad We \ge 2670 \end{aligned} \tag{10}$$

For this case, T can be estimated to be between 4.3 and 5.5, while the breakup time should be about $O(10^{-5})$s. Which verifies the numerical results: initial parent drops are broken up into small drops soon after they enter into the supersonic cross flow.

4.2 Effect of the initial drops size on secondary breakup

In order to further study the secondary breakup effect of the supersonic cross flow on the initial parent droplets, the cases with different initial droplet sizes were investigated, while other conditions were the same as above case.

Fig.2 demonstrates the spray structures with three different initial drops SMR, 35μm, 60μm and 100μm respectively. Fig.4 further shows the quantitative comparison of average spray parameter of three cases, including droplets SMR, velocity, and temperature. It can be found that drop size and penetration of the spray are insensitive to initial drop SMR.

Based on Ref[10], the breakup is envisioned as a multistage process in which fragments will be subject to further breakup as long as the fragments have Weber number exceeding the critical value. A fragment whose Weber number equals the critical Weber number has a diameter equal to the maximum stable diameter. An estimate of the maximum stable diameter was given[10]:

$$d_{stable} = We_{cr}\frac{\sigma}{\rho V_r^2}(1-\frac{V_d}{V_r})^2 \tag{11}$$

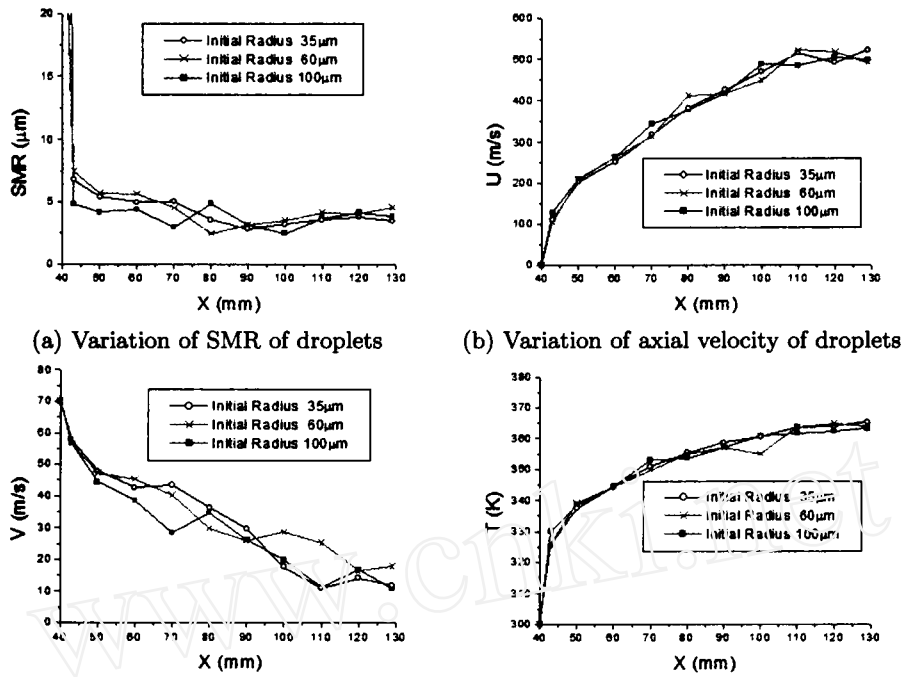

(a) Variation of SMR of droplets (b) Variation of axial velocity of droplets

(c) Variation of transverse velocity of droplets (d) Variation of droplets temperature

Fig. 4. Variation of average spray parameter at the cross section with axial location

Here, Vd is the velocity of the fragment cloud when all breakup processes cease.

$$\frac{V_d}{V_r} = \sqrt{\frac{\rho}{\rho_d}}(\frac{3}{4}C_dT + 3BT^2) \tag{12}$$

From Eq.(10), the dimensionless time T is from 4.3 to 5.5. Then it can be derived that the maximum stable drop diameters with different initial drop size are nearly same magnitude with their relative difference less than 20%.

In summary, the numerical simulation agree with the pilch's experimental and analytical results.

Subsequently, the small drops with same size would almost move in the same manner. As shown in Fig.4(b)-(d), the small drops with different initial drop size have the same variation in the drops temperature and drops velocity. It is further demonstrated in Fig.2 that three kerosene spray plumes have nearly the same penetration.

5 Conclusions

Numerical simulation was conducted to study the kerosene spray characteristics injecting into supersonic cross flow. A stochastic particle method is used to calculate the liquid sprays, in which various sub-models account for the effects of turbulent dispersion, droplet collisions, evaporation and aerodynamic breakup. The corresponding visualization images of the kerosene spray in supersonic combustor were also taken by schlieren to verify the numerical results. It was found that:

1. A bow shock wave was captured upstream of the injector when spray was injected into supersonic cross flow. Meanwhile, Spray is severely bent by the gas flow.

2. During the appropriate range of initial drop size, the parent droplets will be instantaneously broken up into small drops with the same magnitude diameter O(10) micrometers no matter how large the initial drops SMD is. Then the small drops move almost in the same manner.

3. The numerical and experimental kerosene spray plumes showed good agreement.

Acknowledgement

Current research program was supported by the National Science Foundation of China 10102022.

References

1. G. Yu, J.G. Li, X.Y. Zhang, L.H. Chen, C.J. Sung: J. of Propulsion and Power **17(6)**, (2001)
2. L.J. Yue, G. Yu: Journal of Propulsion Technology **25(1)**, (In Chinese)
3. A.A. Amsden, P.J. O'Rourke, T.D. Butler: Los Alamos National Laboratory report LA-11560-MS (1989)
4. R.D. Reitz, C.J. Rutland: Prog. Energy Combust. Sci. **21**, 173 (1995)
5. P.J. O'Rourke, A.A. Amsden: SAE 872089
6. *CFD-ACE Theory Manual*
7. P.G. Simpkins, E.L. Bales: J. Fluid Mech. **55(4)**, 629 (1972)
8. T.-S. Wang: AIAA Paper 2000-2511
9. C.H. Lee, Rolf D.Reitz: International J. of Multiphase Flow **26**, 229 (2000)
10. M. Pilch, C.A. Erdman: International J. of Multiphase Flow **13(6)**, 741 (1987)